Molecular Charge Transfer: A Simple and Effective Route To Engineer the Band Structures of BN Nanosheets and Nanoribbons

ARTICLE *in* THE JOURNAL OF PHYSICAL CHEMISTRY C · SEPTEMBER 2011

Impact Factor: 4.77 · DOI: 10.1021/jp2067205

3 AUTHORS:

Qing Tang
University of California, Riverside
41 PUBLICATIONS **769** CITATIONS
SEE PROFILE

Zhen Zhou
Nankai University
213 PUBLICATIONS **6,996** CITATIONS
SEE PROFILE

Zhongfang Chen
University of Puerto Rico at Rio Piedras
221 PUBLICATIONS **8,056** CITATIONS
SEE PROFILE

THE JOURNAL OF PHYSICAL CHEMISTRY C

ARTICLE

pubs.acs.org/JPCC

Molecular Charge Transfer: A Simple and Effective Route To Engineer the Band Structures of BN Nanosheets and Nanoribbons

Qing Tang,[†,‡] Zhen Zhou,[*,‡] and Zhongfang Chen[*,†]

[†]Department of Chemistry, Institute for Functional Nanomaterials, University of Puerto Rico, Rio Piedras Campus, San Juan, Puerto Rico 00931

[‡]Institute of New Energy Material Chemistry, Key Laboratory of Advanced Energy Materials Chemistry (Ministry of Education), Nankai University, Tianjin 300071, P. R. China

ABSTRACT: The electronic properties of BN nanosheets and nanoribbons doped with organic molecules with strong electron-donating or accepting abilities were investigated by means of density functional theory computations. The interfacial charge transfer between BN nanosheets and the acceptor (tetracyanoquinodimethane, TCNQ) or donor (tetrathiafulvalene, TTF) molecule significantly reduces the intrinsic wide band gap of pristine BN nanosheets and consequently results in a *p*- or *n*-type semiconductor, respectively. Similar behavior is observed for both zigzag and armchair-edged BN nanoribbons. These findings suggest a simple and effective route to tune the electronic properties of BN materials in a wide range and also facilitate the design of BN-based molecular electronics.

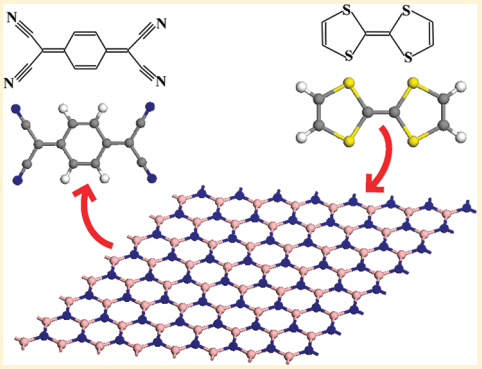

INTRODUCTION

Graphene and its derivatives have exhibited fascinating properties and splendid performances,[1] and the same is expected for novel noncarbon two-dimensional (2D) materials.[2,3] As a structural analogue to graphene, hexagonal BN, a honeycomb network with the C superlattice substituted by B and N atoms, has triggered tremendous research interests.[4,5] The exceptional properties, such as extreme robustness, low density, high chemical stability, and superb thermal conductivity, manifest BN as a promising material in optics and optoelectronic devices.[6]

Compared with carbon-based counterparts, most studies on BN nanomaterials focus on BN nanotubes,[7,8] while BN nanosheets and nanoribbons (BNNRs) have been less explored. This is mainly due to the large difficulty in producing well-defined BN sheets on large scale. However, the challenges confronted in experiments did not deter the enthusiasm of scientists, and impressive progress has been made in the fabrication of BN nanosheets and nanoribbons. Experimentally, 2D BN nanosheets with single or a few atomic layers (two to five layers) have been obtained based on micromechanical cleavage,[9] chemical-derived route,[10] sonication-centrifugation technique,[11,12] bottom-up chemical synthesis,[13] chemical vapor deposition,[14] and liquid exfoliation,[15] and chemical functionalization has been done on the defects.[16] The mono- and few-layer BN nanoribbons were successfully produced by unzipping multiwalled BN nanotubes.[17] The superb properties of BN nanosheets have also been demonstrated; for example, BN nanosheets can considerably improve the thermal and mechanical properties of polymeric composites.[12]

The pristine BN nanosheets, as well as their other morphologies, such as nanotubes and nanoribbons, are intrinsically insulators or wide-band gap semiconductors, which are not ideal for electronic applications. Note that the wide band gap of BN nanomaterials is a severe block in processing BN-based electronics. To tackle this, significant efforts have been made to tailor the band structures of BN nanomaterials. Experimentally, it has been found that the band gap of BN nanotubes can be directly reduced by an electric field,[18] bending deformation,[19] and carbon substitution.[20] Theoretically, various approaches have been proposed to modulate BN nanosheets/nanoribbons, such as C adatom adsorption,[21] electric field application,[22] defect introduction,[23] and surface or edge modification.[24] In particular, Chen et al.[25] predicted that a semiconductor−half metal−metal transition can be realized by precisely controlling the hydrogenation ratio in the hydrogenated zigzag BN nanoribbons.

A promising simple and effective, yet not well-explored method to tune the electronic structure of BN nanosystems, is to form a charge-transfer complex by molecular doping. Compared with other dopants, such as metals, light atoms, and inorganic compounds, organic molecules have several advantages as surface dopants: a large variety of such molecules are available, and new ones can be designed and synthesized; different functional groups can be incorporated into the molecules, which can provide control over the molecular dipole moments, light

Received: July 14, 2011
Revised: August 14, 2011
Published: August 22, 2011

dx.doi.org/10.1021/jp2067205 | *J. Phys. Chem. C* 2011, 115, 18531–18537

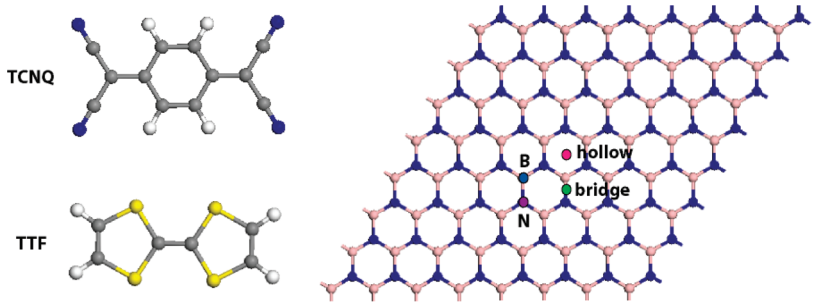

Figure 1. Top views of the molecular structures for TCNQ and TTF dopants (left) and the supercell of 8 × 8 × 1 BN sheet (right), with the possible doping sites specified by four circular symbols in different colors.

sensing properties, hydrophilic or hydrophobic characters, and so forth.

So far, the surface doping by organic molecules has been used to modulate the electronic properties of graphene.[26−29] For example, the Raman spectroscopy and electronic structure of graphene are markedly affected by the interaction with electron -donating and -accepting molecules such as aniline and nitrobenzene.[28] Chen et al.[29] revealed that the surface electron transfer from graphene to the adsorbed tetrafluorotetracyanoquinodimethane (F_4-TCNQ) is responsible for the *p*-doping of epitaxial graphene grown on 6H-SiC (0001).

The same effect is expected on BN and other noncarbon 2D nanomaterials. However, to our best knowledge, there is no theoretical or experimental report on the noncovalent surface doping via organic molecules on BN nanosheets/nanoribbons. In this work, by means of density functional theory (DFT) computations, we investigated the effects of doping BN nanosheets/nanoribbons with organic molecules of effective electron -donating and -withdrawing capabilities, namely, tetrathiafulvalene (TTF) and TCNQ. Our results indicate that the doping behaviors on the BN nanosheets and nanoribbons are almost the same: in both cases, they can be turned into *p*- or *n*-type semiconductors by adsorbing acceptor (TCNQ) or donor (TTF) molecules, respectively.

COMPUTATIONAL METHOD

The selected dopants are TTF, an excellent electron donor, and TCNQ, a strong electron acceptor, both of which are widely used as building blocks of charge transfer salts and have drawn deep interest in the field of molecular electronics.[30]

All of the DFT computations were carried out by using the Vienna ab initio simulation package (VASP). The ion−electron interaction is described with the projected augmented wave (PAW)[31] method. The exchange-correlation energy is described by the functional of Perdew, Burke, and Ernzerhof (PBE)[32] based on the generalized gradient approximation (GGA). In all computations, the electron wave functions were expanded in plane waves with an energy cutoff of 400 eV. The total energy computations were performed by using 8 × 8 × 1 and 1 × 1 × 5 Monkhorst-Pack *k*-point grid for BN nanosheets and nanoribbons, respectively. The geometry optimizations were performed by using the conjugated gradient method, and the convergence threshold was set to be 10^{-4} eV in energy and 10^{-3} eV/Å in force. The larger *k*-point grids (24 × 24 × 1 and 1 × 1 × 21 *k* points for BN nanosheets and nanoribbons, respectively) were used for band structure computations.

To study the adsorption of TCNQ and TTF molecule on the BN sheet, an 8 × 8 × 1 BN supercell containing 64 B and 64 N atoms was adopted. The nearest distance between two TCNQ (TTF) molecules in adjacent supercells is ∼10 Å, and a vacuum separation of 14 Å was used to ensure negligible interaction between the organic molecules and the BN sheet in the adjacent unit cell. For BNNRs, the 8-zigzag (with width of 16.0 Å) and 14-armchair (with width of 16.2 Å) nanoribbons are chosen as the representative models, with the two bare edges terminated by H atoms. The model is composed of 1 × 1 × 6 and 1 × 1 × 4 supercell for 8-zigzag and 14-armchair BNNRs, respectively. This leads to the separation of at least 8 Å for the molecule and its image in adjacent supercells.

RESULTS AND DISCUSSION

Charge-Transfer Complexes of BN Nanosheets. The doping molecules are initially placed parallel to the BN monolayer surface with a vertical distance of 3.1 Å, significantly larger than the sum of the corresponding atomic van der Waals radii. Four different adsorption sites are considered, with the molecular center lying directly atop the B or N atoms, the B−N bridge center, and the central hollow ring (Figure 1).

The energetically most favorable geometries for the complexes between BN sheet and TCNQ/TTF are illustrated in Figure 2 parts a and b, respectively. No chemical bonds form between these interactive species. In both complexes, the in-plane B−N bonds or intramolecular bonds of TCNQ (TTF) change negligibly, and the bond lengths also differ very slightly (<0.004 Å). Thus, the interaction between these organic dopants and BN substrate is mostly governed by the weak dipole−dipole and electrostatic forces.

In the lowest-energy configuration (Figure 2a), TCNQ floats above the BN layer with a height of about 3.49 Å; meanwhile, the BN sheet is slightly crumpled from the flat plane (with a variation of 0.14 Å). In comparison, the separation between TTF and BN sheet is elongated to 3.68 Å, and TTF is severely bent (the central C atoms are 0.45 Å away from the plane defined by the four rim H atoms, Figure 2b). The adsorption of TTF also results in a serious distortion of the BN sheet, and the rumpling of BN plane increases to ∼0.32 Å.

Note that the energy differences between the most favorable and the less favorable doping sites are very small, in the range of 3.9−6.5 meV for TCNQ and 2.6−58.6 meV for TTF, respectively. Thus, the energy barrier for the molecular migration can be easily overcome, and both TCNQ and TTF are subject to be easily mobile on the BN surface if an appropriate external perturbation occurs.

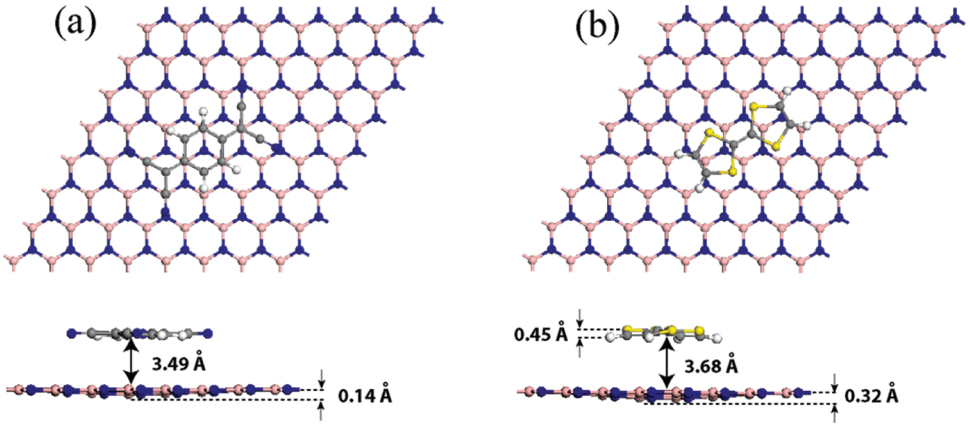

Figure 2. Top and side views of the lowest-energy configurations of the complexes between BN sheet and TCNQ (a) and TTF (b). The distance between the dopants and the BN sheet as well as the bending magnitude from the planar molecular or BN plane is also given.

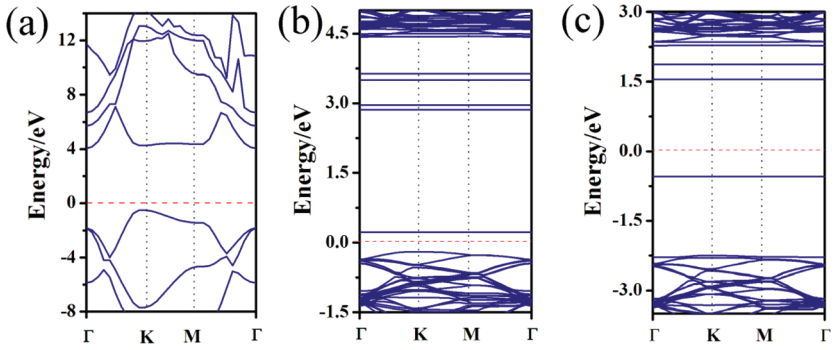

Figure 3. Band structures of pristine BN sheet (a), TCNQ-BN (b), and TTF-BN (c). The Fermi level is set to be zero and indicated by the red dotted line.

The binding energy per molecule is determined by $\Delta E = E_{\text{mol-BN}} - (E_{\text{BN}} + E_{\text{mol}})$, where $E_{\text{mol-BN}}$, E_{BN}, and E_{mol} stand for the total energy of the molecule-BN system, the isolated BN sheet, and the single molecule, respectively. By this definition, a more negative ΔE denotes a more favorable interaction. For TCNQ and TTF in its most stable configuration, the computed ΔE is −0.112 and −0.041 eV, respectively. This indicates that the adsorption process of TCNQ/TTF on BN surface is exothermic, and TCNQ has a stronger interaction with BN sheet than TTF. Thus, the formation of such complexes is predicted to be experimentally feasible from an energetic perspective. Note that the GGA functional tends to underestimate the binding energies of weak interactions; however, the basic mechanism and physical essence behind these interactive species should not change, which are our major concerns. The real system should have a stronger binding, and the adsorbed molecules can be stabilized on the BN surface.

To examine how these doping molecules affect the electronic properties of BN nanosheets, we computed the electronic band structures for BN sheet before and after doping (Figure 3). The pristine BN sheet is a wide-band gap semiconductor with a band gap of 4.78 eV, in good agreement with previous report.[5d] However, in the doped BN systems, several flat sub-bands emerge within the wide band of the pristine BN sheet; consequently the band gap is decreased to 0.43 and 2.07 eV for the TCNQ and TTF complexes, respectively.

However, the origin for band modifications is drastically different in these two types of complexes. The band structure of a doped BN sheet can be roughly considered as a simple combination of the band structures of BN sheet and the dopant, due to the weak interaction between them. For the BN system decorated by the typical electron acceptor, TCNQ, the conduction band minimum (CBM) is derived from the lowest unoccupied molecular orbital (LUMO) of TCNQ, and the valence band maximum (VBM) comes from the BN sheet. This can also be confirmed by a detailed analysis on the partial density of states (PDOS) (Figure 4a): the introduced new state above the highest valence band is mainly ascribed to the TCNQ molecule. The charge transfer from the BN sheet to TCNQ is 0.12 |e| by Hirshfeld charge analysis. Thus, the adsorption of electrophilic molecule turns the BN sheet into a *p*-type semiconductor. This is analogous to a theoretical report by He et al.[33] that a *p*-type semiconductor can be obtained by encapsulating electrophilic organic molecules into BN nanotubes. On the other hand, for the nucleophilic TTF molecule, which acts as an electron donor, both its highest occupied molecular orbital (HOMO) and LUMO correspond to the VBM and CBM of the doped BN system, respectively (see the PDOS in Figure 4b). The resulting band gap is significantly reduced (2.07 eV, Figure 3c), which transforms the TTF-BN system into an *n*-type semiconductor. The charge transfer from the nucleophilic TTF to the BN substrate is about 0.06 |e| per molecule, a little smaller than that for the TCNQ situation.

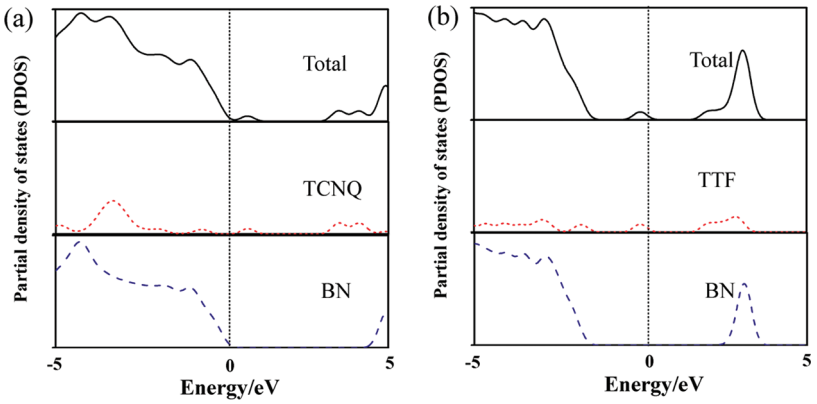

Figure 4. Total density of states (top) and partial density of states (PDOS) for the TCNQ (a) and TTF (b) doped BN sheet. The PDOS is projected on the individual dopant (middle) and the BN substrate (bottom), respectively.

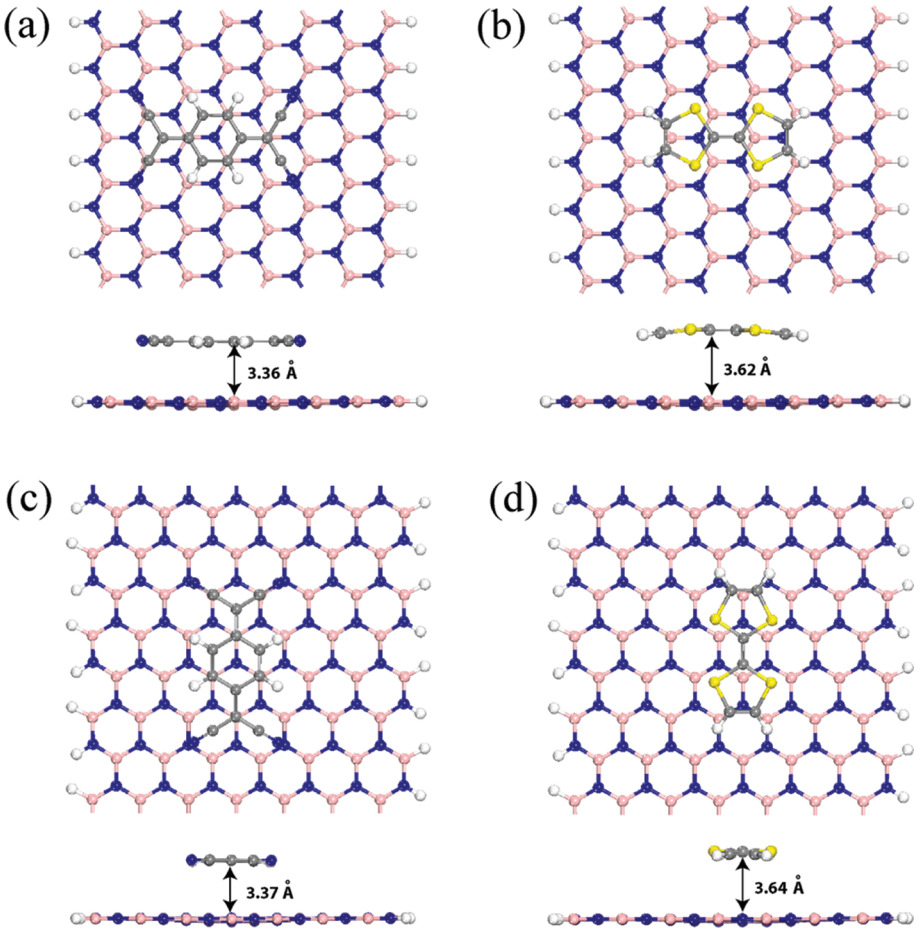

Figure 5. Optimized geometries of the TCNQ doped 8-zigzag (a) and 14-armchair (c) BNNRs, as well as the TTF doped 8-zigzag (b) and 14-armchair (d) BNNRs.

Charge-Transfer Complexes of BN Nanoribbons. We also examined the molecule doping on the BNNRs, and both zigzag and armchair-edged BNNRs were considered. The optimized geometries and band structures of the TCNQ/TTF doped 8-zigzag and 14-armchair nanoribbons are displayed in Figures 5 and 6, respectively.

Our computations revealed that the doped configurations of both 8-zigzag and 14-armchair BNNRs bear much structural resemblance to the parent BN sheet, and their electronic properties are also significantly modified. For the 8-zigzag BNNR, the band gap drops from 4.23 to 0.48 eV and 1.98 eV after surface doping by acceptor (TCNQ) and donor (TTF) molecules. Similarly, the band gap of 14-armchair decreases from 4.55 to 0.49 eV and 2.01 eV by molecule doping. The binding energies of TCNQ (TTF) on 8-zigzag and 14-armchair BNNRs are 0.107 eV (0.009 eV) and 0.135 eV (0.047 eV), respectively. The charge

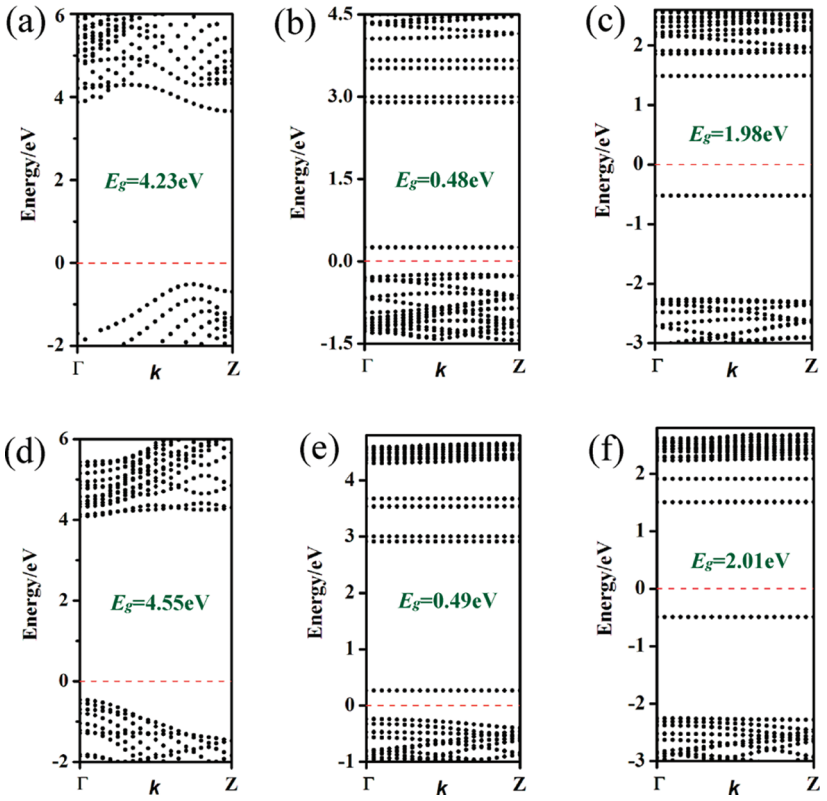

Figure 6. Band structures of the pristine 8-zigzag BNNR (a), along with its complex with TCNQ (b) and TTF (c). In accordance, parts d−f are for the 14-armchair BNNR case. The band gap is shown in the corresponding band structure.

transfer from 8-zigzag and 14-armchair BNNRs to TCNQ is 0.12|e| and 0.11|e|, respectively, while the charge transfer from TTF to 8-zigzag and 14-armchair BNNRs is 0.01|e| and 0.09|e|, respectively. These results on BNNRs are nearly comparable to what we obtained for the BN nanosheet. Clearly, with doping by TCNQ and TTF, both 8-zigzag and 14-armchair BNNRs are converted into a *p*-type and *n*-type semiconductor, respectively, and the band gap reduction is also expected for wider zigzag or armchair BN ribbons.

CONCLUSION AND PROSPECTS

In this work, we carried out a theoretical study on the electronic properties of functionalized BN nanosheet/nanoribbons by surface doping with organic molecules. Because of the charge transfer, the surface doping of strong electron acceptor (TCNQ) or donor (TTF) molecules can significantly reduce the band gap of the pristine BN nanosheet/nanoribbons and convert the originally wide-band gap semiconductor into a *p*- or *n*-type semiconductor. The charge transfer through noncovalent molecular doping permits an effective band engineering of the BN nanosheet/nanoribbons without destroying the sp^2 structural integrity.

The two organic dopants studied here are only two representatives of the large quantities of electron-donor or acceptor molecules. It is expected that the band structure of BN systems can be adjusted by doping with different organic molecules in a desired manner. With molecule doping, the modification of BN surface with patterned donor and acceptor molecules may be useful to achieve *p*−*n* junctions, which are the basic building units of many semiconductor electronic devices, such as diodes, transistors, solar cells, and integrated circuits.

Besides BN, we are highly optimistic that forming charge-transfer complexes is a good option for the band engineering of other wide-band gap 2D nanosystems, such as TiO_2, ZnO, CdS, CdSe, GaAs, and Si. We hope that further theoretical and experimental work will confirm these appealing predictions.

AUTHOR INFORMATION

Corresponding Author

*E-mail: zhouzhen@nankai.edu.cn (Z.Z.); zhongfangchen@gmail.com (Z.C.).

ACKNOWLEDGMENT

Support in China by NSFC (21073096), MOE NCET (08-0293), and Innovation Research Team (IRT0927) and in the United States by NSF Grant EPS-1010094 and the NASA grant (Nos. NNX10AM80H, NNX07AO30A) is gratefully acknowledged.

REFERENCES

(1) (a) Novoselov, K. S.; Geim, A. K.; Morozov, S. V.; Jiang, D.; Zhang, Y.; Dubonos, S. V.; Grigorieva, I. V.; Firsov, A. A. Electric Field Effect in Atomically Thin Carbon Films. *Science* **2004**, *306*, 666–669. (b) Zhang, Y.; Tan, Y.; Stormer, H. L.; Kim, P. Experimental Observation of the Quantum Hall Effect and Berry's Phase in Graphene. *Nature* **2005**, *438*, 201–204. (c) Geim, A. K.; Novoselov, K. S. The rise of graphene. *Nat. Mater.* **2007**, *6*, 183–191.

(2) Novoselov, K. S.; Jiang, D.; Schedin, F.; Booth, T. J.; Khotkevich, V. V.; Morozov, S. V.; Geim, A. K. Two-Dimensional Atomic Crystals. *Proc. Natl. Acad. Sci. U.S.A.* **2005**, *102*, 10451–10453.

(3) For recent reviews, see(a) Castro Neto, A. H.; Novoselov, K. Two-Dimensional Crystals: Beyond Graphene. *Mater. Express* **2011**, *1*, 10–17. (b) Mas-Ballesté, R.; Gómez-Navarro, C.; Gómez-Herrero, J.; Zamora, F. 2D Materials: To Graphene and Beyond. *Nanoscale* **2011**, *3*, 20–30.

(4) (a) Paine, R. T.; Narula, C. K. Synthetic Routes to Boron Nitride. *Chem. Rev.* **1990**, *90*, 73–91. (b) Kubota, Y.; Watanabe, K.; Tsuda, O.; Taniguchi, T. Deep Ultraviolet Light-emitting Hexagonal Boron Nitride Synthesized at Atmospheric Pressure. *Science* **2007**, *317*, 932–934. (c) Watanabe, K.; Taniguchi, T.; Kanda, H. Direct-bandgap Properties and Evidence for Ultraviolet Lasing of Hexagonal Boron Nitride Single Crystal. *Nat. Mater.* **2004**, *3*, 404–409. (d) Corso, M.; Auwärter, W.; Muntwiler, M.; Tamai, A.; Greber, T.; Osterwalder, J. Boron Nitride Nanomesh. *Science* **2004**, *303*, 217–220. (e) Golberg, D.; Bando, Y.; Huang, Y.; Terao, T.; Mitome, M.; Tang, C.; Zhi, C. Boron Nitride Nanotubes and Nanosheets. *ACS Nano* **2010**, *4*, 2979–2993.

(5) (a) Arnaud, B.; Lebègue, S.; Rabiller, P.; Alouani, M. Huge Excitonic Effects in Layered Hexagonal Boron Nitride. *Phys. Rev. Lett.* **2006**, *96*, 026402. (b) Liu, L.; Feng, Y. P.; Shen, Z. X. Structural and Electronic Properties of *h*-BN. *Phys. Rev. B* **2003**, *68*, 104102. (c) Xu, Y. N.; Ching, W. Y. Calculation of Ground State and Optical Properties of Boron Nitrides in the Hexagonal, Cubic, and Wurtzite Structures. *Phys. Rev. B* **1991**, *44*, 7787–7798. (d) Topsakal, M.; Aktürk, E.; Ciraci, S. First-principles Study of Two- and One-dimensional Honeycomb Structures of Boron Nitride. *Phys. Rev. B* **2009**, *79*, 115442.

(6) (a) Blase, X.; Rubio, A.; Louie, S. G.; Cohen, M. L. Stability and Band-Gap Constancy of Boron-Nitride Nanotubes. *Europhys. Lett.* **1994**, *28*, 335–340. (b) Chen, Y.; Zou, J.; Campbell, S. J.; Caer, G. L. Boron Nitride Nanotubes: Pronounced Resistance to Oxidation. *Appl. Phys. Lett.* **2004**, *84*, 2430–2432.

(7) (a) Yan, B.; Park, C.; Ihm, J.; Zhou, G.; Duan, W.; Park, N. Electron Emission Originated from Free-Electron-like States of Alkali-Doped Boron-Nitride Nanotubes. *J. Am. Chem. Soc.* **2008**, *130*, 17012–17015. (b) Liu, R.; Li, J.; Zhou, G.; Wu, J.; Gu, B.; Duan, W. Formation, Morphology, and Effect of Complex Defects in Boron Nitride Nanotubes: An ab initio Calculation. *J. Phys. Chem. C* **2011**, *115*, 12782–12788. (c) Hao, S.; Zhou, G.; Duan, W.; Wu, J.; Gu, B. Transverse Pressure Induced Phase Transitions in Boron Nitride Nanotube Bundles and the Lightest Boron Nitride Crystal. *J. Am. Chem. Soc.* **2008**, *130*, 5257–5261. (d) Hao, S.; Zhou, G.; Duan, W.; Wu, J.; Gu, B. Tremendous Spin-Splitting Effects in Open Boron Nitride Nanotubes: Application to Nanoscale Spintronic Devices. *J. Am. Chem. Soc.* **2006**, *128*, 8453–8458. (e) Wu, X.; An, W.; Zeng, X. C. Chemical Functionalization of Boron-Nitride Nanotubes with NH_3 and Amino Functional Groups. *J. Am. Chem. Soc.* **2006**, *128*, 12001–12006.

(8) (a) Zhi, C.; Bando, Y.; Tang, C.; Golberg, D. Immobilization of Proteins on Boron Nitride Nanotubes. *J. Am. Chem. Soc.* **2005**, *127*, 17144–17145. (b) Wei, X.; Wang, M.; Bando, Y.; Golberg, D. Post-Synthesis Carbon Doping of Individual Multiwalled Boron Nitride Nanotubes via Electron-Beam Irradiation. *J. Am. Chem. Soc.* **2010**, *132*, 13592–13593. (c) Zhi, C.; Bando, Y.; Wang, W.; Tang, C.; Kuwahara, H.; Golberg, D. Molecule Ordering Triggered by Boron Nitride Nanotubes and "Green" Chemical Functionalization of Boron Nitride Nanotubes. *J. Phys. Chem. C* **2007**, *111*, 18545–18549. (d) Gao, Z.; Zhi, C.; Bando, Y.; Golberg, D.; Serizawa, T. Noncovalent Functionalization of Disentangled Boron Nitride Nanotubes with Flavin Mononucleotides for Strong and Stable Visible-Light Emission in Aqueous Solution. *ACS Appl. Mater. Interfaces* **2011**, *3*, 627–632. (e) Tang, C.; Bando, Y.; Huang, Y.; Yue, S.; Gu, C.; Xu, F. F.; Golberg, D. Fluorination and Electrical Conductivity of BN Nanotubes. *J. Am. Chem. Soc.* **2005**, *127*, 6552–6553. (f) Gao, Z.; Zhi, C.; Bando, Y.; Golberg, D.; Serizawa, T. Isolation of Individual Boron Nitride Nanotubes via Peptide Wrapping. *J. Am. Chem. Soc.* **2010**, *132*, 4976–4977. (g) Terao, T.; Zhi, C.; Bando, Y.; Mitome, M.; Tang, C.; Golberg, D. Alignment of Boron Nitride Nanotubes in Polymeric Composite Films for Thermal Conductivity Improvement. *J. Phys. Chem. C* **2010**, *114*, 4340–4344. (h) Tang, C.; Bando, Y.; Ding, X.; Qi, S.; Golberg, D. Catalyzed Collapse and Enhanced Hydrogen Storage of BN Nanotubes. *J. Am. Chem. Soc.* **2002**, *124*, 14550–14551. (i) Horváth, L.; Magrez, A.; Golberg, D.; Zhi, C.; Bando, Y.; Smajda, R.; Horváth, E.; Forró, L.; Schwaller, B. In Vitro Investigation of the Cellular Toxicity of Boron Nitride Nanotubes. *ACS Nano* **2011**, *5*, 3800–3810.

(9) (a) Pacile, D.; Meyer, J. C.; Girit, C. O.; Zettl, A. The Two-dimensional Phase of Boron Nitride: Few-atomic-layer Sheets and Suspended Membranes. *Appl. Phys. Lett.* **2008**, *92*, 133107. (b) Gorbachev, R. V.; Riaz, I.; Nair, R. R.; Jalil, R.; Britnell, L.; Belle, B. D.; Hill, E. W.; Novoselov, K. S.; Watanabe, K.; Taniguchi, T.; Geim, A. K.; Blake, P. Hunting for Monolayer Boron Nitride: Optical and Raman Signatures. *Small* **2011**, *7*, 465–468.

(10) (a) Han, W.; Wu, L.; Zhu, Y.; Watanabe, K.; Taniguchi, T. Structure of Chemically Derived Mono- and Few-atomic Layer Boron Nitride Sheets. *Appl. Phys. Lett.* **2008**, *93*, 223103. (b) Warner, J. H.; Rümmeli, M. H.; Bachmatiuk, A.; Büchner, B. Atomic Resolution Imaging and Topography of Boron Nitride Sheets Produced by Chemical Exfoliation. *ACS Nano* **2010**, *4*, 1299–1304.(c) Pakdel, A.; Zhi, C.; Bando, Y.; Nakayama, T.; Golberg, D. Boron Nitride Nanosheet Coatings with Controllable Water Repellency. *ACS Nano* **2011**, DOI: 10.1021/nn201838w. (d) Wang, X.; Zhi, C.; Li, L.; Zeng, H.; Li, C.; Mitome, M.; Golberg, D.; Bando, Y. Chemical Blowing" of Thin-Walled Bubbles: High-Throughput Fabrication of Large-Area, Few-Layered BN and C_x-BN Nanosheets. *Adv. Mater.* **2011**, DOI: 10.1002/adma.201101788.

(11) Lin, Y.; Williams, T. V.; Xu, T. B.; Cao, W.; Elsayed-Ali, H. E.; Connell, J. W. Aqueous Dispersions of Few-Layered and Monolayered Hexagonal Boron Nitride Nanosheets from Sonication-Assisted Hydrolysis: Critical Role of Water. *J. Phys. Chem. C* **2011**, *115*, 2679–2685.

(12) Zhi, C.; Bando, Y.; Tang, C.; Kuwahara, H.; Golberg, D. Large scale fabrication of boron nitride nanosheets and their utilization in polymeric composites with improved thermal and mechanical properties. *Adv. Mater.* **2009**, *21*, 2889–2893.

(13) Nag, A.; Raidongia, K.; Hembram, K. P. S. S.; Datta, R.; Waghmare, U. V.; Rao, C. N. R. Graphene Analogues of BN: Novel Synthesis and Properties. *ACS Nano* **2010**, *4*, 1539–1544.

(14) Song, L.; Ci, L.; Lu, H.; Sorokin, P. B.; Jin, C.; Ni, J.; Kvashnin, A. G.; Kvashnin, D. G.; Lou, J.; Yakobson, B. I.; Ajayan, P. M. Large Scale Growth and Characterization of Atomic Hexagonal Boron Nitride Layers. *Nano Lett.* **2010**, *10*, 3209–3215.

(15) (a) Lin, Y.; Williams, T. V.; Connell, J. W. Soluble, Exfoliated Hexagonal Boron Nitride Nanosheets. *J. Phys. Chem. Lett.* **2010**, *1*, 277–283. (b) Coleman, J. N.; Lotya, M.; O'Neill, A.; Bergin, S. D.; King, P. J.; Khan, U.; Young, K.; Gaucher, A.; De, S.; Smith, R. J.; Shvets, I. V.; Arora, S. K.; Stanton, G.; Kim, H. Y.; Lee, K.; Kim, G. T.; Duesberg, G. S.; Hallam, T.; Boland, J. J.; Wang, J. J.; Donegan, J. F.; Grunlan, J. C.; Moriarty, G.; Shmeliov, A.; Nicholls, R. J.; Perkins, J. M.; Grieveson, E. M.; Theuwissen, K.; McComb, D. W.; Nellist, P. D.; Nicolosi, V. Two-dimensional nanosheets produced by liquid exfoliation of layered materials. *Science* **2011**, *331*, 568–571.

(16) Lin, Y.; Williams, T. V.; Cao, W.; Elsayed-Ali, H. E.; Connell, J. W. Defect Functionalization of Hexagonal Boron Nitride Nanosheets. *J. Phys. Chem. C* **2010**, *114*, 17434–17439.

(17) (a) Zeng, H.; Zhi, C.; Zhang, Z.; Wei, X.; Wang, X.; Guo, W.; Bando, Y.; Golberg, D. "White Graphenes": Boron Nitride Nanoribbons via Boron Nitride Nanotube Unwrapping. *Nano Lett.* **2010**, *10*, 5049–5055.(b) Erickson, K. J.; Gibb, A. L.; Sinitskii, A.; Rousseas, M.; Alem, N.; Tour, J. M.; Zettl, A. K. Longitudinal Splitting of Boron Nitride Nanotubes for the Facile Synthesis of High Quality Boron Nitride Nanoribbons. *Nano Lett.* **2011**, DOI: 10.1021/nl2014857.

(18) Ishigami, M.; Sau, J. D.; Aloni, S.; Cohen, M. L.; Zettl, A. Observation of the Giant Stark Effect in Boron-Nitride Nanotubes. *Phys. Rev. Lett.* **2005**, *94*, 056804.

(19) Bai, X. D.; Golberg, D.; Bando, Y.; Zhi, C. Y.; Tang, C. C.; Mitome, M.; Kurashima, K. Deformation-Driven Electrical Transport of Individual Boron Nitride Nanotubes. *Nano Lett.* **2007**, *7*, 632–637.

(20) Wei, X.; Wang, M.; Bando, Y.; Golberg, D. Electron-Beam-Induced Substitutional Carbon Doping of Boron Nitride Nanosheets, Nanoribbons, and Nanotubes. *ACS Nano* **2011**, *5*, 2916–2922.

(21) Li, J.; Zhou, G.; Chen, Y.; Gu, B.-L.; Duan, W. H. Magnetism of C Adatoms on BN Nanostuctures: Implications for Functional Nanodevices. *J. Am. Chem. Soc.* **2009**, *131*, 1796–1801.

(22) (a) Zhang, Z.; Guo, W. Energy-Gap Modulation of BN Ribbons by Transverse Electric Fields: First-Principles Calculations. *Phys. Rev. B* **2008**, *77*, 075403. (b) Park, C.; Louie, S. G. Energy Gaps and Stark Effect in Boron Nitride Nanoribbons. *Nano Lett.* **2008**, *8*, 2200–2203.

(23) (a) Si, M. S.; Xue, D. S. Magnetic Properties of Vacancies in a Graphitic Boron Nitride Sheet by First-Principles pseudopotential calculations. *Phys. Rev. B* **2007**, *75*, 193409. (b) Si, M. S.; Li, J. Y.; Shi, H. G.; Niu, X. N.; Xue, D. S. Divacancies in Graphitic Boron Nitride Sheets. *Eur. Phys. Lett.* **2009**, *86*, 46002. (c) Azevedo, S.; Kaschny, J. R.; de Castilho, C. M. C.; de Brito Mota, F. A Theoretical Investigation of Defects in a Boron Nitride Monolayer. *Nanotechnology* **2007**, *18*, 495707. (d) Bhowmick, S.; Singh, A. K.; Yakobson, B. I. Quantum Dots and Nanoroads of Graphene Embedded in Hexagonal Boron Nitride. *J. Phys. Chem. C* **2011**, *115*, 9889–9893. (e) Chen, W.; Li, Y.; Yu, G.; Zhou, Z.; Chen, Z. Electronic Structure and Reactivity of Boron Nitride Nanoribbons with Stone-Wales Defects. *J. Chem. Theory Comput.* **2009**, *5*, 3088–3095. (f) Yin, L.; Cheng, H.; Saito, R. Triangle Defect States of Hexagonal Boron Nitride Atomic Layer: Density Functional Theory Calculations. *Phys. Rev. B* **2010**, *81*, 153407. (g) Du, A.; Chen, Y.; Zhu, Z.; Amal, R.; Lu, G. Q.; Smith, S. C. Dots versus Antidots: Computational Exploration of Structure, Magnetism, and Half-Metallicity in Boron-Nitride Nanostructures. *J. Am. Chem. Soc.* **2009**, *131*, 17354–17359.

(24) (a) Ataca, C.; Ciraci, S. Functionalization of BN honeycomb structure by adsorption and substitution of foreign atoms. *Phys. Rev. B* **2010**, *82*, 165402. (b) Gao, X. F.; Zhou, Z.; Zhao, Y. L.; Nagase, S.; Zhang, S. B.; Chen, Z. Comparative Study of Carbon and BN Nanographenes: Ground Electronic States and Gap Energy Engineering. *J. Phys. Chem. C* **2008**, *112*, 12677–12682. (c) Terrones, M.; Charlier, J.-C.; Gloter, A.; Cruz-Silva, E.; Terrés, E.; Li, Y. B.; Vinu, A.; Dominguez, J. M.; Terrones, H.; Bando, Y.; Golberg, D. Experimental and Theoretical Studies Suggesting the Possibility of Metallic Boron Nitride Edges in Porous Nanourchins. *Nano Lett.* **2008**, *8*, 1026–1032. (d) Wu, X.; Wu, M.; Zeng, X. C. Chemically Decorated Boron-Nitride Nanoribbons. *Front. Phys. China* **2009**, *4*, 367–372. (e) Tang, S.; Cao, Z. Structural and electronic properties of the fully hydrogenated boron nitride sheets and nanoribbons: Insight from first-principles calculations. *Chem. Phys. Lett.* **2010**, *488*, 67–72. (f) Liu, Y.; Wu, X.; Zhao, Y.; Zeng, X. C.; Yang, J. Half-Metallicity in Hybrid Graphene/Boron Nitride Nanoribbons with Dihydrogenated Edges. *J. Phys. Chem. C* **2011**, *115*, 9442–9450.

(25) Chen, W.; Li, Y.; Yu, G.; Li, C.; Zhang, S. B.; Zhou, Z.; Chen, Z. Hydrogenation: A Simple Approach To Realize Semiconductor-Half-Metal-Metal Transition in Boron Nitride Nanoribbons. *J. Am. Chem. Soc.* **2010**, *132*, 1699–1705.

(26) (a) Coletti, C.; Riedl, C.; Lee, D. S.; Krauss, B.; Patthey, L.; von Klitzing, K.; Smet, J. H.; Starke, U. Charge neutrality and band-gap tuning of epitaxial graphene on SiC by molecular doping. *Phys. Rev. B* **2010**, *81*, 235401. (b) Voggu, R.; Das, B.; Rout, C. S.; Rao, C. N. R. Effects of charge transfer interaction of graphene with electron donor and acceptor molecules examined using Raman spectroscopy and cognate techniques. *J. Phys.: Condens. Matter* **2008**, *20*, 472204.

(27) (a) Sun, J. T.; Lu, Y. H.; Chen, W.; Feng, Y. P.; Wee, A. T. S. Linear tuning of charge carriers in graphene by organic molecules and charge-transfer complexes. *Phys. Rev. B* **2010**, *81*, 155403. (b) Pinto, H.; Jones, R.; Goss, J. P.; Briddon, P. R. P-type doping of graphene with F4-TCNQ. *J. Phys.: Condens. Matter* **2009**, *21*, 402001. (c) Lu, Y. H.; Chen, W.; Feng, Y. P.; He, P. M. Tuning the Electronic Structure of Graphene by an Organic Molecule. *J. Phys. Chem. B* **2009**, *113*, 2–5.

(28) Das, B.; Voggu, R.; Rout, C. S.; Rao, C. N. R. Changes in the Electronic Structure and Properties of Graphene Induced by Molecular Charge-transfer. *Chem. Commun.* **2008**, 5155–5157.

(29) Chen, W.; Chen, S.; Qi, D. C.; Gao, X. Y.; Wee, A. T. S. Surface Transfer p-Type Doping of Epitaxial Graphene. *J. Am. Chem. Soc.* **2007**, *129*, 10418–10422.

(30) (a) Rovira, C. Bis(ethylenethio)tetrathiafulvalene (BET-TTF) and Related Dissymmetrical Electron Donors: From the Molecule to Functional Molecular Materials and Devices (OFETs). *Chem. Rev.* **2004**, *104*, 5289–5317. (b) Metzger, R. M. Electrical Rectification by a Molecule: The Advent of Unimolecular Electronic Devices. *Acc. Chem. Res.* **1999**, *32*, 950–957.

(31) Blöchl, P. E. Projector Augmented-wave Method. *Phys. Rev. B* **1994**, *50*, 17953–17979.

(32) Perdew, J. P.; Burke, K.; Ernzerhof, M. Generalized Gradient Approximation Made Simple. *Phys. Rev. Lett.* **1996**, *77*, 3865–3868.

(33) He, W.; Li, Z.; Yang, J.; Hou, J. G. A First Principles Study on Organic Molecule Encapsulated Boron Nitride Nanotubes. *J. Chem. Phys.* **2008**, *128*, 164701.